ELSEVIER

Biochimica et Biophysica Acta 1463 (2000) 209–218

BIOCHIMICA ET BIOPHYSICA ACTA
BBA

www.elsevier.com/locate/bba

Effects of the hinge region of cecropin A(1–8)–magainin 2(1–12), a synthetic antimicrobial peptide, on liposomes, bacterial and tumor cells

Song Yub Shin [a], Joo Hyun Kang [a], So Yun Jang [a], Yangmee Kim [b], Kil Lyong Kim [a], Kyung-Soo Hahm [a,*]

[a] *Peptide Engineering Research Unit, Korea Research Institute of Bioscience and Biotechnology, P.O. Box 115, Yusong, Taejon 305-600, South Korea*

[b] *Department of Chemistry, Konkuk University, Seoul 143-701, South Korea*

Received 28 June 1999; received in revised form 5 October 1999; accepted 5 October 1999

Abstract

A 20-residue hybrid peptide (CA(1–8)–MA(1–12): KWKLFKKIGIGKFLHSAKKF–NH_2) incorporating 1–8 residues of cecropin A (CA) and 1–12 residues of magainin 2 (MA) has potent antibiotic activity without hemolytic activity. In order to investigate the effects of the flexible hinge sequence, Gly–Ile–Gly of CA(1–8)–MA(1–12) (CA–MA) on antibiotic activity, CA–MA and its three analogues, CA–MA1, CA–MA2 and CA–MA3 were synthesized. The Gly–Ile–Gly sequence of CA–MA was deleted in CA–MA1 and replaced with Pro and Gly–Pro–Gly in CA–MA2 and CA–MA3, respectively. CA–MA1 and CA–MA3 caused a significant decrease in the bactericidal rate against *Escherichia coli* and *Bacillus subtilis* and the tumoricidal activity against four different tumor cells, and the PC/PS (4:1, w/w) vesicle-aggregating and disrupting activities. However, CA–MA2 showed a similar bactericidal rate and antitumor, vesicle-aggregating and disrupting activities, as compared with CA–MA. These results suggested that the flexibility or β-turn induced by Gly–Ile–Gly or Pro in the central part of CA–MA may be important in the electrostatic interaction of the cationic short α-helical region in the N-terminus with the cell membrane surface and the hydrophobic interaction of amphipathic α-helical region in the C-terminus with the hydrophobic acyl chains in the cell membrane. CA–MA3 exhibited lower activity in antibacterial, antitumor, and vesicle-aggregating and disrupting activities than CA–MA and CA–MA2. This result suggested that the excessive β-turn structure by Gly–Pro–Gly in CA–MA3 seems to interrupt the ion channel/pore formation on the lipid bilayer. It was concluded that the appropriate flexibility or β-turn structure provided by the central hinge is responsible for the effective antibiotic activity of the antimicrobial peptides with the helix–hinge–helix structure.

Keywords: Cecropin A(1–8)–magainin 2(1–12); Hinge region; Antibiotic activity

1. Introduction

In recent years, the antimicrobial peptides have become recognized as an important component of the non-specific host defense system and innate immunity of insects, amphibians, and mammals. Cecropin A (CA), one of the first reported peptides of these antimicrobial peptides, is found in the hemolymph of *Hyalophora cecropia* pupae and consists of 37 amino acid residues [1–5]. Magainin 2 (MA), a 23-amino acid antimicrobial peptide, is identified from the skin of the African clawed frog *Xenopus*

* Corresponding author. Fax: +82-42-860-4593; E-mail: hahmks@kribb4680.kribb.re.kr

0005-2736/00/$ – see front matter
PII: S0005-2736(99)00210-2

Table 1
Amino acid sequences of CA–MA and its analogues

Peptide	Amino acid sequence	Remarks
CA–MA	KWKLFKKIGIGKFLHSAKKF-NH_2	CA(1–8)–MA(1–12)
CA–MA1	KWKLFKKI——KFLHSAKKF-NH_2	CA(1–8)–MA(1–12):$G^9I^{10}G^{11}$ deletion
CA–MA2	KWKLFKKI−P−KFLHSAKKF-NH_2	CA(1–8)–MA(1–12):$G^9I^{10}G^{11} \rightarrow P$
CA–MA3	KWKLFKKIGPGKFLHSAKKF-NH_2	CA(1–8)–MA(1–12): $I^{10} \rightarrow P$

laevis [6–9]. CA and MA display strong bacteriolytic activity against Gram-positive and Gram-negative bacteria, but have no toxicity against normal eukaryotic cells such as erythrocytes [4,7–9]. The antibacterial activity of these two peptides has been related to their ability to adopt an amphipathic α-helical conformation. Melittin (ME), a 26-residue peptide derived from honey bee venom, shows powerful antibacterial properties, but is very cytotoxic (e.g., hemolytic) for normal eukaryotic cells [10,11]. The recent emergence of drug resistant bacteria, fungi, and parasites has resulted in a considerable interest in using endogenous antimicrobial peptides as therapeutic agents.

Peptide antibiotics as therapeutic agents should act against a very wide range of bacterial cells but have no cytotoxicity on normal eukaryotic cells. In the course of systematic studies aimed at finding antibiotic peptides having improved antibacterial activity without toxic effect on normal eukaryotic cells such as erythrocytes, a series of CA–ME hybrid peptides composed from the N-terminal cationic amphipathic region of CA and the N-terminal hydrophobic region of ME were synthesized [11–13]. These CA–ME hybrid peptides displayed more effective antibacterial activity than parental CA and less toxicity against erythrocytes than ME [11–13]. In our previous study, CA(1–8)–ME(1–12), one of these hybrid peptides, was found to have effective antibacterial activity, but is very hemolytic at high peptide concentration (e.g., 100 μM).

Also in our previous study, CA(1–8)–MA(1–12) (CA–MA), composed of the amino terminal sequence of CA and MA, was found to display similar antibacterial and antitumor activities, as compared with CA(1–8)–ME(1–12), but it showed no hemolytic activity until 100 μM [14–17]. CA(1–8)–MA(1–12) (CA–MA) and CA(1–8)–ME(1–12) (CA–ME) are composed of an N-terminal cationic, a short α-helix and a C-terminal amphipathic α-helix joined by a flexible hinge sequence of Gly^9–Ile^{10}–Gly^{11}. The cationic amphipathic helix–hinge–hydrophobic helix arrangement is a common structural motif found in the antimicrobial peptides such as CA, cecropin B(CB), and pardaxin [17–23]. Cationicity and amphipathicity of these peptides are believed to facilitate initial electrostatic contact with polyanionic sites in the wall or membrane of the target microorganism and are essential for the membrane-disruptive ability [24–34]. However, the effects of the hinge region of these peptides on antibiotic activity against bacterial and tumor cells have not yet been investigated.

Therefore, in the present study, the effects of the deletion (CA–MA1) and substitution with Pro (CA–MA2), a helix breaker or Gly–Pro–Gly (CA–MA3), a β-turn inducer at the flexible hinge sequence (Gly^9–Ile^{10}–Gly^{11}) in CA–MA on the antibacterial, antitumor, and vesicle-aggregating and disrupting activities were investigated (Table 1). The vesicle-disrupting activities of the peptides were investigated by the measurement of released dye from dye-encapsulating vesicles. Human erythrocyte and a mouse fibroblast cell line were used to measure the cytotoxicity of the peptides against normal eukaryotic cells. The secondary structures of the peptides were investigated by circular dichroism (CD) in the membrane-mimicking environment, such as trifluoroethanol (TFE), sodium dodecyl sulfate (SDS).

2. Materials and methods

2.1. Peptide synthesis and purification

The peptides were synthesized by the solid phase method [35] using Fmoc(9-fluorenylmethoxycarbonyl)-chemistry (Table 1). Rink Amide 4-methylbenzhydryl-amine (MBHA) resin (0.55 mmol/g) was

used as the support to obtain a C-terminal amidate peptide. The coupling of Fmoc-amino acids was performed with *N*-hydroxybenzotriazole (HOBt) and dicyclohexylcarbodiimide (DCC). Amino acid side chains were protected as follows: *t*-butyl (Ser and Thr), trityl (His), *t*-butyloxycarbonyl (Lys). Deprotection and cleavage from the resin were carried out using a mixture of trifluoroacetic acid, phenol, water, thioanisole, 1,2-ethanedithiol and triisopropylsilane (82.5:5:5:5:2.5:2, v/v) for 2 h at room temperature. The crude peptide was then repeatedly washed with diethylether, and dried in a vacuum. The crude peptides were purified by a reversed-phase preparative HPLC on a Waters 15-μm Deltapak C_{18} column (19×30 cm). Purity of the purified peptides was confirmed by analytical reversed-phase HPLC on an Ultrasphere C_{18} column (Beckman, USA), 4.6×25 cm. The purified peptides were hydrolyzed with 6 N HCl at 110°C for 22 h, and then dried in a vacuum. The residues were dissolved in 0.02 N HCl and subjected to an amino acid analyzer (Hitachi Model 8500 A, Japan). The amino acid composition of the synthetic peptides was confirmed by amino acid analysis. The molecular masses of the synthetic peptides were determined with MALDI (matrix-assisted laser desorption/ionization) mass spectra.

2.2. Hemolytic activity

The hemolytic activity of the peptides was evaluated by determining hemoglobin release of 4% suspensions of fresh human erythrocytes at 414 nm. Human red blood cells were centrifuged and washed three times with phosphate-buffered saline (PBS: 35 mM phosphate buffer/0.15 M NaCl, pH 7.0). One hundred μl of human red blood cells suspended 8% (v/v) in PBS were plated into 96-well plates, and then 100 μl of the peptide solution was added to each well. The plates were incubated for 1 h at 37°C, and centrifuged at 150×*g* for 5 min. One-hundred-μl aliquots of the supernatant were transferred to 96-well plates. Hemolysis was measured by absorbance at 414 nm with an ELISA plate reader (Molecular Devices Emax, Sunnyvale, CA, USA). Zero percent hemolysis and 100% hemolysis were determined in PBS and 0.1% Triton-X 100, respectively. The hemolysis percentage was calculated using the following equation: % hemolysis = [($Abs_{414\,nm}$ in the peptide solution − $Abs_{414\,nm}$ in PBS)/($Abs_{414\,nm}$ in 0.1% Triton X-100 − $Abs_{414\,nm}$ in PBS)]×100.

2.3. Antibacterial activity

Escherichia coli (KCTC cat. no. 1682), *Salmonella typhimurium* (KCTC cat. no. 1926), *Pseudomonas aeruginosa* (KCTC cat. no. 1637), *Bacillus subtilis* (KCTC cat. no. 1918), *Streptococcus pyogenes* (KCTC cat. no. 3096), and *Staphylococcus aureus* (KCTC cat. no. 1621) were supplied by the Korean Collection for Type Cultures (KCTC), Korea Research Institute of Bioscience and Biotechnology (Taejon, Korea). The bacteria were grown to the mid-logarithmic phase in a medium (g/l) (10 bactotryptone/5 yeast extract/10 NaCl (pH 7.0)). The peptides were stepwise-diluted in a medium of 1% bactopeptone. The tested organism (final bacterial suspension: 2×10^6 colony formation units (CFU)/ml) suspended in growth medium (100 μl) was mixed with 100 μl of the test peptide solution in a microtiter plate well with three replicates for each test solution. Microbial growth was determined by the increase in optical density at 620 nm after 10 h incubation at 37°C. The minimal inhibitory concentration (MIC) was defined as the lowest concentration of peptide at which there was no change in optical density.

2.4. Growth inhibitory activity on tumor cells and normal cell

Growth inhibitory activity of the peptides against cancer and normal fibroblast cells was determined as 50% inhibition concentration (IC_{50}) using a tetrazolium (MTT) colorimetric assay. Human chronic myelogenous leukemia (K-562: ATCC cat. no. CCL-243), human acute T-cell leukemia (Jurkat: ATCC cat. no. TIB-152), human lung carcinoma cancer cells (K-549: ATCC cat. no. CCL-185) and human breast adenocarcinoma cell (MDA-MB-361: ATCC cat. no. HTB-27) were used for the growth inhibitory activity assay of the peptides against cancer cells. Mouse NIH-3T3 fibroblast cell (ATCC cat. no. CRL-1658) were used for growth inhibitory activity assay of the peptides against normal cells. These cells were obtained from the Genetic Resources Center of Korea Research Institute of Bioscience and Biotechnology (Taejon, Korea). The cells were grown in a RPMI-

1640 medium supplemented with 10% heat-inactivated fetal bovine serum (FBS), 100 units/ml penicillin G sodium, and 100 μg/ml streptomycin sulfate. The cells were plated on 96 well plates at a density of 2.0×10^4 cells/well in 150 μl of the same medium. After incubating the plates overnight at 37°C in 5% CO_2 atmosphere, 20 μl of serially diluted peptides were added and then incubated for 3 days. Twenty μl of MTT solution (5 mg/ml MTT in phosphate-buffered saline) was added to each well and the plates were incubated at 37°C for 4 h. Forty μl of 20% SDS solution containing 0.02 M HCl was added to dissolve the dark-blue crystals which formed (MTT-formazan product) in each well, and then incubated overnight. Absorbance was measured at 570 nm on an ELISA plate reader (Molecular Devices Emax).

2.5. Kinetics of bacterial killing

The kinetics of bacterial killing of the peptides were evaluated using *E. coli* and *B. subtilis*. Log-phase bacteria (6×10^5 CFU/ml) were incubated with 2.5 μM peptide in LB broth. Aliquots were removed at fixed time intervals, appropriately diluted, plated on LB broth agar plate, and then the colony-forming units were counted after 16–18 h incubation at 37°C.

2.6. Determination of vesicle aggregation

Phospholipid vesicle aggregating activity of the peptides was measured by the changes in turbidity at 400 nm using a Beckman DU-8 spectrophotometer (Palo Alto, CA, USA). Phospholipid vesicle suspension composed of phosphatidylcholine (PC)/phosphatidylserine (PS) (4:1, w/w) was prepared in Hepes buffer (10 mM Hepes, 150 mM NaCl, pH 7.4) to give a final concentration of 35 μM by the sonication process [36]. Various amounts of the peptides were added to the vesicle suspension to obtain various ratios of peptide to phospholipid.

2.7. Carboxyfluorescein leakage measurements

Carboxyfluorescein (CF)-encapsulated large unilamellar vesicles (LUV) composed of PC/PS (4:1, w/w) were prepared by the reversed-phase ether evaporation method [37] using 100 mM CF. The initially formed vesicles were extruded through Nucleopore filter of 0.1 μm. To remove free CF dye, the vesicles were passed through a Bio-Gel A 0.5m (Bio-Rad, Richmond, USA) column (1.5×30 cm) using phosphate-buffered saline (pH 7.4) as the eluting buffer. The separated LUV fraction, after appropriate dilution to a final concentration of 6.36 μM, was mixed with the peptide solution in a 2 ml cuvette at 25°C. The leakage of CF from the LUV was monitored by measuring fluorescence intensity at 520 nm excited at 490 nm on a Shimadzu RF-5000 spectrofluorometer (Tokyo, Japan). The apparent percent leakage value at a fluorescence intensity, F, was calculated by the following equation:

$$\%\ \text{leakage (apparent)} = 100\times(F-F_0)/(F_t-F_0)$$

F_t denotes the fluorescence intensity corresponding to 100% leakage after the addition of 20 μl of 10% Triton X-100. F_0 represents the fluorescence of the intact vesicle.

2.8. Circular dichroism (CD) spectroscopy

CD spectra of peptides were recorded using a Jasco J720 spectropolarimeter using a 1 mm pathlength cell (Japan). The CD spectra of the peptides in 10 mM sodium phosphate buffer (pH 7.2), 50% (v/v) TFE, or 30 mM SDS were recorded at 25°C in the 190–240 nm wavelength range at 0.1-nm intervals. The peptide concentrations were 100 μg/ml. The mean residue ellipticity $[\theta]$ was calculated using the molecular mass of each peptide as determined from the amino acid composition. The percentage helicity of the peptides were calculated with the equation [38]: $\%\ \text{helix} = 100([\theta]_{222}-[\theta]^0_{222})/[\theta]^{100}_{222}$, where $[\theta]_{222}$ is the observed mean residue ellipticity per residue at 222 nm in deg•cm^2 dmol^{-1}. $[\theta]^0_{222}$ and $[\theta]^{100}_{222}$ are the estimated ellipticities corresponding to a random coil (-1000 deg•cm^2 dmol^{-1}) and 100% helical peptides ($-36\,500$ deg•cm^2 dmol^{-1}), respectively.

3. Results

3.1. Antibacterial, antitumor and hemolytic activity

Antibacterial activity of the peptides was deter-

mined as minimal inhibitory concentration (MIC) value against Gram-positive and Gram-negative bacterial strains (Table 2). All peptides completely inhibited the growth of all bacteria strains tested with MIC values from 0.78 to 6.25 μM. As shown in Table 2, the deletion (CA–MA1) and Pro (CA–MA2) or Gly–Pro–Gly substitution (CA–MA3) of Gly–Ile–Gly sequence in CA–MA had no significant effect on bactericidal activity after long-time incubation. Since CA–MA and its analogues show similar MIC values on bacterial strains tested, the time course of the peptides to kill mid-logarithmic phase of *E. coli* and *B. subtilis* were compared. As shown in Fig. 1, CA–MA and CA–MA2 displayed faster bactericidal rate against both *E. coli* and *B. subtilis* than CA–MA1 and CA–MA3. These results indicate that the Gly–Ile–Gly hinge sequence or β-turn inducing Pro residue in the central region of CA–MA have an important role in the bactericidal rate against both *E. coli* and *B. subtilis*. The excessive flexible β-turn structure induced by Gly–Pro–Gly substitution in the central hinge region of CA–MA brought about a drastic reduction in the bactericidal rate for *E. coli* and *B. subtilis*. This fact suggests that the appropriate flexibility in the central hinge region of CA–MA is more responsible for the bactericidal rate against *E. coli* and *B. subtilis* than bactericidal activity.

The cytotoxicity against normal eukaryotic cells of the peptides was measured by monitoring the hemoglobin released from incubating 4% human red blood cell suspension with 100 μM peptide. None of the peptides exhibited any hemolytic activity below 100 μM. The IC_{50} of the peptides on the four different tumor cells were obtained from the plots of cell survival (%) versus the concentration of the peptides (Fig. 2). The IC_{50} values of the peptides against the four different tumor cells are summarized in Table 2. The deletion and Gly–Pro–Gly substitution of Gly–Ile–Gly in CA–MA caused a significant reduction in the tumoricidal activity against tumor cells. In addition, CA–MA2 with Pro substitution in the hinge region of CA–MA showed a 1.5–2.0 times greater tumoricidal activity than CA–MA.

All the peptides displayed higher IC_{50} values (>100 μM) in growth inhibition against normal NIH-3T3 fibroblast cells (Table 2). The significant difference in growth inhibitory activity of all the peptides between normal and transformed eukaryotic cells may be due to the outer membrane surface of transformed tumor cells having more exposed anionic lipids than that of normal cells.

3.2. Peptide-induced vesicle aggregation and disruption

To elucidate the peptide-induced dye leakage out

Table 2
Antibacterial, antitumor and hemolytic activities of CA–MA and its analogues

Cell types		CA–MA	CA–MA1	CA–MA2	CA–MA3
Gram-negative bacteria (MIC: μM)	*E. coli*	3.125	6.25	6.25	3.125
	S. typhimurium	0.78	0.78	0.78	0.78
	P. aeruginosa	1.56	1.56	3.125	0.78
Gram-positive bacteria (MIC: μM)	*B. subtilis*	0.78	1.56	1.56	0.78
	S. pyogenes	0.78	0.78	0.78	0.78
	S. aureus	3.125	3.125	3.125	3.125
Tumor cells (IC_{50}: μM)	K-562	65.0	85.3	35.1	>100
	A-549	60.0	100	25.0	>100
	Jurkat	30.0	65.0	20.0	75.0
	MDA-MB-361	44.0	100	28.0	>100
Normal cell (IC_{50}: μM)	NIH-3T3 fibroblast	>100	>100	>100	>100
% Hemolysis (100 μM)	Human erythrocytes	0	0	0	0

Minimal inhibitory concentrations were determined by incubating approximately 2×10^6 CFU/ml of cells with serial dilutions of a 96-well microtiter plate. Bacterial growth was assessed optical density measurement at 620 nm. The lowest concentration of the peptides that any suppression of bacterial growth was defined MIC. The 50% inhibition concentration (IC_{50}) of the peptides against NIH-3T3 fibroblast cell and four tumor cells was determined using the MTT assay. Hemolytic activity of each peptide was determined using human erythrocytes. The release of hemoglobin was monitored by measuring the optical density at 414 nm, as compared with that of the cell suspension treated with 0.1% Triton X-100, was defined % hemolysis.

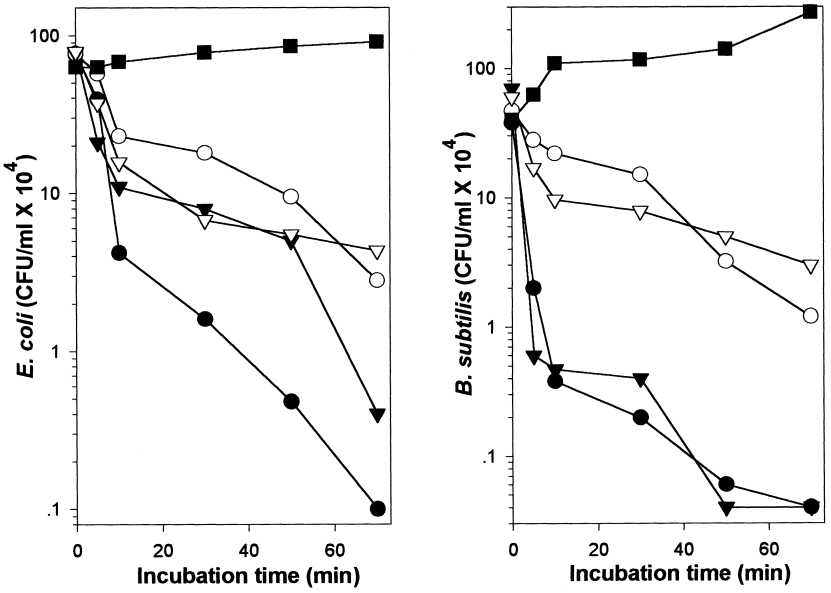

Fig. 1. Kinetics of killing *E. coli* and *B. subtilis* by CA–MA and its analogues. Bacteria, either untreated (■) or treated with 2.5 μM CA–MA (●), 2.5 μM CA–MA1 (○), 2.5 μM CA–MA2 (▼), or 2.5 μM CA–MA3 (▽), were diluted at the indicated time intervals, and then plated on LB broth agar. The colony-forming units were calculated by counting the plates after 16–18 h incubation at 37°C.

of phospholipid vesicles, the vesicle aggregation event was examined as the initial step in the peptide–vesicle interaction process. The changes in vesicle size due to aggregation could be monitored by the absorbance of vesicle suspension at 400 nm. The light scattering intensity is known to be quite sensitive to particle size. Fig. 3 showed the changes in absorbance at 400 nm as a function of concentration of the added peptide to the PC/PS (4:1, w/w) vesicle. When CA–MA2 was added to the PC/PS vesicle solution, a sharper increase and a higher absorbance intensity due to effective aggregation was observed. These aggregation events induced by peptides might result from the interaction of negatively-charged PS and these cationic peptides. This suggestion was supported by the results that these peptides did not induce the aggregation of PC vesicle, zwitterionic phospholipid, and the aggregation efficiencies were dependent on the PS content of the used vesicle (Fig. 3, inset).

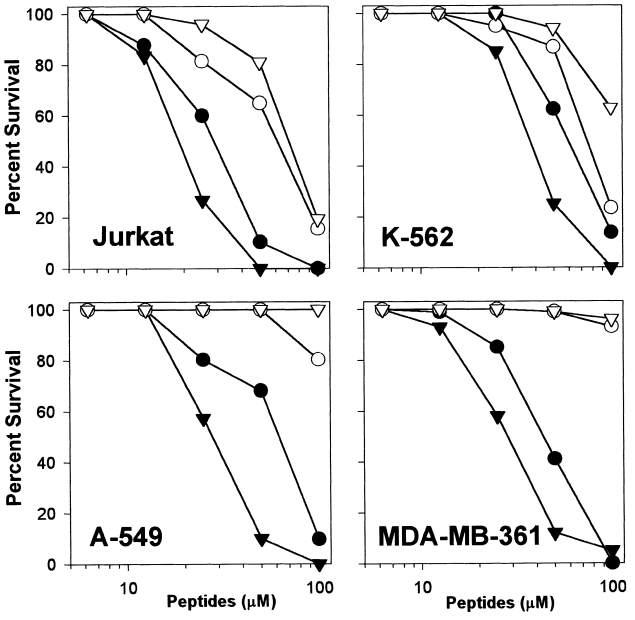

Fig. 2. Concentration–response curves of CA–MA (●), CA–MA1 (○), CA–MA2 (▼) and CA–MA3 (▽) in growth inhibition against three different transformed tumor cells.

The interaction of the peptides with phospholipid vesicles was further investigated by measuring the ability of the peptides to perturb the PC/PS (4:1) LUV (Fig. 4). CA–MA2, the most effective peptide in inducing vesicle aggregation, exhibited the highest activity in the vesicle disruption (Fig. 4). This result suggested that the relative efficiencies of these peptides to perturb the lipid membranes were correlated with their vesicle aggregation activities. The release of CF from the vesicle was dependent on the concentration of peptides in the vesicle suspension. The ex-

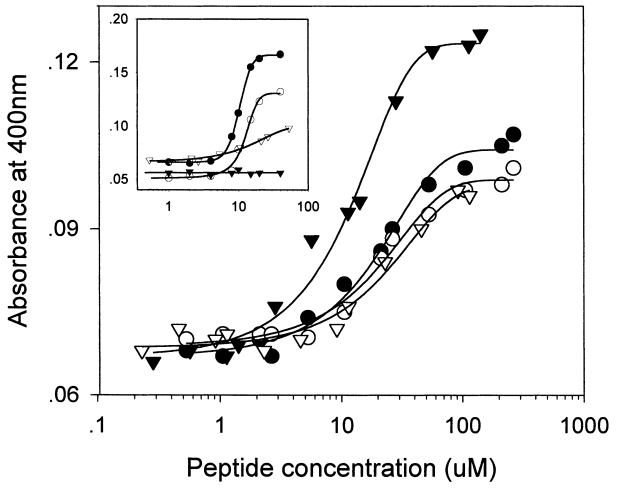

Fig. 3. Monitoring the phospholipid vesicle (PC/PS = 4:1, w/w) aggregation induced by peptides. The vesicle aggregation was determined by measuring the absorbance at 400 nm in 10 mM Hepes buffer containing 150 mM NaCl (pH 7.4). (●) CA–MA; (○) CA–MA1; (▼) CA–MA2; (▽) CA–MA3. Inset: the aggregation efficiency of phospholipid vesicle depending on the PS content induced by CA–MA. (●) PS vesicle; (○) PC/PS (1:1, w/w) vesicle; (▽) PC/PS (4:1, w/w) vesicle; (▼) PC vesicle.

tent of CF release induced by CA–MA as a function of peptide to lipid molar ratio (P/L) was found to be a sigmoidal pattern (Fig. 4, inset), but those of other peptides were hyperbolic curves. This might indicate that an accumulation of CA–MA is involved in the CA–MA-induced vesicle leakage process.

In order to investigate the membrane-interacting mechanisms of CA–MA and its analogues, the vesicle aggregation and perturbation activities by peptides were observed with the PC/PS (4:1) vesicle as the artificial model membrane. These peptides induced not only the aggregation but also the perturbation of vesicles in a dose-dependent manner. The importance of electrostatic interactions in the peptide–lipid vesicle was suggested by the results that CA–MA and its analogues specifically induced the aggregation of the vesicle containing negatively-charged phospholipid and the reduced aggregation efficiency by the addition of zwitterionic PC to PS membrane. The aggregation efficiency of phospholipid vesicle by CA–MA increased in the order to PS vesicle > PC/PS (1:1, w/w) vesicle > PC/PS (4:1, w/w) ≫ PC vesicle (Fig. 3, inset). When the peptide was added to phospholipid vesicle solution, the positively charged region of the peptide was electrostatically attracted to the negatively charged head group of acidic phospholipid, PS and then the membrane-induced α-helical region might penetrate the lipid bilayer.

3.3. Peptide structural analysis

Many antimicrobial peptides including cecropins and magainins adapt the α-helical structure in membrane-mimetic environments such as TFE, SDS micelles or liposome [27–31]. The CD spectra of the peptides were measured in phosphate buffer with or without the α-helix inducing solvent TFE or SDS composed of an aliphatic tail and a negatively charged head group mimicked the lipid membrane. As shown in Fig. 5, the CD spectrum indicated that CA–MA and its analogues have random coil conformations in phosphate buffer, while form a well-defined α-helical structure in the presence of 50% TFE and 30 mM SDS. All the peptides showed higher α-helical content in 50% TFE than 30 mM SDS (Fig. 5, Table 3).

In 50% TFE solution, the deletion of Gly–Ile–Gly (CA–MA1) in CA–MA did not affect the α-helical content. In contrast, it resulted in about a twofold

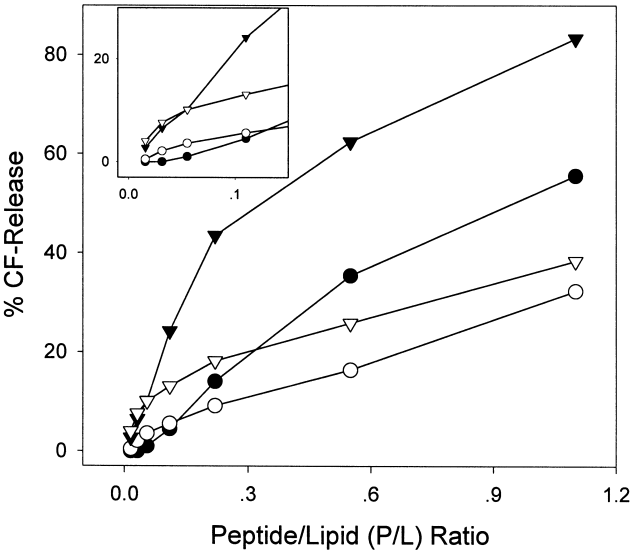

Fig. 4. Release of CF from LUVs composed of PC/PS (4:1, w/w). The extents of vesicle disruption induced by peptide were indicated as a function of peptide to lipid ratio (P/L). The released CF fluorescence was measured at $\lambda_{ex} = 490$ nm and $\lambda_{em} = 520$ nm. Inset: the %CF release at low P/L ratio. (●) CA–MA; (○) CA–MA1; (▼) CA–MA2; (▽) CA–MA3.

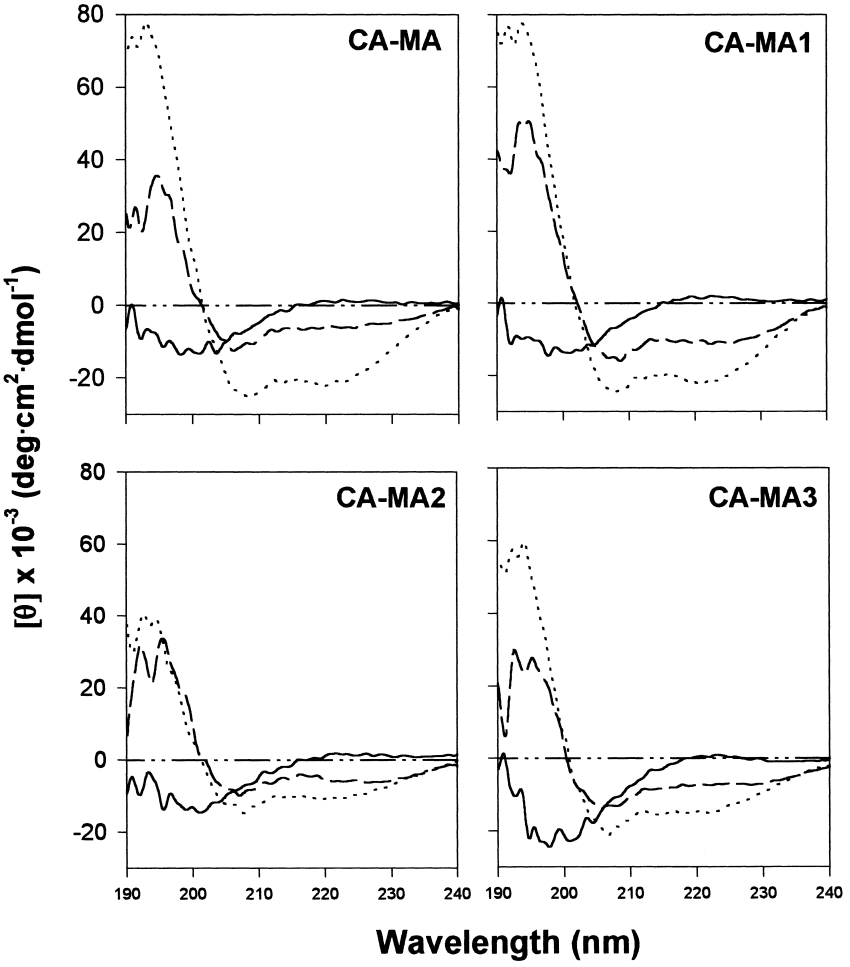

Fig. 5. CD spectra of CA–MA and its analogues in the solutions of 30 mM SDS (dashed line), 0 (solid line), and 50% (v/v) TFE (dotted line), respectively, containing 10 mM sodium phosphate buffer, pH 7.2.

increase of α-helical content in 30 mM SDS micelle. Substitution of Pro (CA–MA2) for Gly–Ile–Gly in CA–MA caused about a twofold decrease in α-helical content in both 50% TFE and 30 mM SDS solution. Substitution of Gly–Pro–Gly (CA–MA3) for Gly–Ile–Gly in CA–MA resulted in a slight increase of α-helical content in SDS micelle. Nevertheless, none of all the peptides showed a significant difference in α-helical content in cell membrane mimicking environment such as TFE solution and SDS micelles,

Table 3
Percent α-helicity of CA–MA and its analogues in various solution

Peptide	Buffer		50% TFE		30 mM SDS	
	$[\theta]_{222}$	α-helix (%)	$[\theta]_{222}$	α-helix (%)	$[\theta]_{222}$	α-helix (%)
CA–MA	1170	5.9	−20 860	54.4	−6140	14.1
CA–MA1	1930	8.0	−21 450	56.0	−11 080	27.6
CA–MA2	1800	7.7	−10 450	28.9	−5 810	13.2
CA–MA3	420	3.9	−15 040	38.5	−7 470	17.7

The percent α-helicity of the peptides were calculated with the equation: % helix = $100([\theta]_{222}-[\theta]^{0}_{222})/[\theta]^{100}_{222}$.

they had different lytic abilities against bacterial and tumor cells. This indicates that the α-helical structural characteristic of the peptide may play an important role in killing bacterial and tumor cells, but its α-helical content may not be correlated to their antibacterial and antitumor activities.

4. Discussion

The hybrid peptide, CA–MA, was found to have effective antibacterial activity against Gram-positive and Gram-negative bacterial strains and even potent antitumor activity against some transformed tumor cells, but it had no hemolytic effect for human erythrocytes [14–17]. Unlike CA and CB with amphipathic helix–flexible–hydrophobic helix motif, CA–MA has the structural motif of the cationic short helix–flexible–amphipathic helix. In our previous study, the Gly–Ile–Gly sequence in the tertiary structure of CA–MA in an aqueous 50% TFE solution determined by two-dimensional NMR study was observed to be rather flexible [39]. This flexible sequence in the central region of CA–MA is thought to play an important role in antibiotic activity against bacterial and tumor cells and disrupting ability for artificial lipid bilayers. Therefore, in this study, the effect of the flexible Gly–Ile–Gly sequence of CA–MA on its antibiotic activity against bacterial and tumor cells and the vesicle-aggregating and disrupting abilities was investigated.

Deletion of Gly–Ile–Gly (CA–MA1) and substitution of Gly–Pro–Gly (CA–MA3) in CA–MA did not affect antibacterial activity (MIC value) against Gram-positive and Gram-negative bacterial strains induced by long-term peptide incubation. In contrast, CA–MA1 and CA–MA3 resulted in a significant decrease in the bactericidal rate against *E. coli* and *B. subtilis* and the tumoricidal activity against the four different transformed cancer cells, and the PC/PS vesicle-aggregating and disrupting activities. However, CA–MA2 with Pro residue instead of Gly–Ile–Gly sequence of CA–MA showed similar antitumor activity, and bactericidal rate against *E. coli* and *B. subtilis* and PC/PS vesicle-aggregating and disrupting activities when compared with CA–MA.

The Gly–Ile–Gly and Pro in the tertiary structure of CA–MA and CA–MA2 in dodecylphosphocholine (DPC) micelles determined by two-dimensional NMR analysis was found to have almost similar flexibility (unpublished data). Accordingly, these results suggested that the flexibility or bent potential induced by Gly–Ile–Gly sequence or Pro residue in the central part of CA–MA may be important in the electrostatic interaction of the cationic short α-helical region in the N-terminus with the cell membrane surface and the hydrophobic interaction of amphipathic α-helical region in the C-terminus with the hydrophobic acyl chains in the cell membrane. CA–MA3 exhibited lower activity in antibacterial, antitumor, and vesicle-aggregating and disrupting activities than CA–MA and CA–MA2. This result suggests that the extended turn structure provided by Gly–Pro–Gly in CA–MA3 seems to interrupt the ion channel/pore formation on the cell membrane. Also, in our previous study, the substitution of Gly–Pro–Gly for Gly–Ile–Gly in CA(1–13)–MA(1–13) and CA(1–13)–ME(1–13) hybrid peptides resulted in a drastic reduction in both antibacterial and antitumor activity [17]. In contrast, the substitutions of Gly–Pro, Pro, or Gly–Ile for Gly–Ile–Gly of CA–MA analogue (L–CA–MA: KWKLFKKI-GIGFLHLAKKF–NH_2) retained good antibacterial and antitumor activity [17].

Therefore, our results indicated that appropriate flexibility or bend potential provided by Gly–Pro, Pro, or Gly–Ile for Gly–Ile–Gly in the central hinge region which connects the cationic α-helical N-terminus and the amphipathic α-helical C-terminus of the antimicrobial peptides is responsible for their effective antibacterial and antitumor activity with no or less cytotoxicity against normal eukaryotic cells. The lytic activity induced by CA–MA and its analogues was less effective for the normal cells than for tumor cells. It was reported that the anionic phospholipids such as phospatidylserine (PS) in the outer membrane leaflet of human tumor cells is highly exposed [40].

Also, as shown in Fig. 4, the vesicle-aggregation activity of CA–MA increased with increasing of PS content of the phospholipid vesicle. Therefore, the difference in cytotoxic effect of CA–MA and its analogues between tumor and normal cells is due to the peptides interacting strongly with the anionic phospholipids on the cell surface of the tumor cells. This

interpretation may be supported by Chen et al.'s study [41]: CB-1 having more positive charged residues was more effective for HL-60, K-562, Jurkat and CCRF-CEB leukemia cancer cells than CB. Accordingly, these results suggest that the electrostatic attraction of the peptides to the anionic phospholipids on the cell surface may be one of the main driving forces before lysis in membrane bilayers can be efficiently initiated.

Acknowledgements

This work was supported by a grant (NB 1140) from the Ministry of Science and Technology, South Korea.

References

[1] H. Steiner, D. Hultmark, A. Engstr, H. Bennich, H.G. Boman, Nature 292 (1981) 246–248.
[2] J.Y. Lee, A. Boman, C. Sun, M. Andersson, H. Jornvall, V. Mutt, H.G. Boman, Proc. Natl. Acad. Sci. USA 86 (1989) 9159–9162.
[3] P. von Hofsten, I. Faye, K. Kockum, J.Y. Lee, K.G. Xanthopouls, A. Boman, G. Boman, A. Engstrom, D. Andreu, R.B. Merrifield, Proc. Natl. Acad. Sci. USA 82 (1985) 2240–2243.
[4] H.G. Boman, Cell 65 (1991) 205–207.
[5] H.G. Boman, I. Fay, G.H. Gudmundsson, J.-Y. Lee, D.-A. Lidholm, Eur. J. Biochem. 201 (1991) 23–31.
[6] M. Zasloff, Proc. Natl. Acad. Sci. USA 84 (1987) 5449–5453.
[7] C.L. Bevins, M. Zasloff, Annu. Rev. Biochem. 59 (1990) 395–414.
[8] H.G. Boman, Annu. Rev. Immunol. 13 (1995) 61–92.
[9] W.L. Maloy, U.P. Kari, Biopolymers (Pept. Sci.) 37 (1995) 105–112.
[10] M.T. Tosteson, S.J. Holmes, M. Razin, D.C. Tosteson, J. Membr. Biol. 87 (1985) 35–44.
[11] H.G. Boman, D. Wade, A. Boman, B. Wahlin, R.B. Merifield, FEBS Lett. 259 (1989) 103–106.
[12] D. Andreu, J. Ubach, A. Boman, D. Wahlin, D. Wade, R.B. Merrifield, H.G. Boman, FEBS Lett. 296 (1992) 190–194.
[13] D. Wade, D. Andreu, S.A. Mitchell, A.M.V. Silveira, A. Boman, H.G. Boman, R.B. Merrifield, Int. J. Pept. Protein Res. 40 (1992) 429–436.
[14] S.Y. Shin, M.K. Lee, K.L. Kim, K.-S. Hahm, J. Pept. Res. 50 (1997) 279–285.
[15] S.Y. Shin, J.H. Kang, M.K. Lee, S.Y. Kim, Y. Kim, K.-S. Hahm, Biochem. Mol. Biol. Int. 44 (1998) 1119–1126.
[16] J.H. Kang, S.Y. Shin, S.Y. Jang, M.K. Lee, K.-S. Hahm, J. Pept. Res. 52 (1998) 45–50.
[17] S.Y. Shin, J.H. Kang, K.-S. Hahm, J. Pept. Res. 53 (1999) 82–90.
[18] Y. Shai, D. Bach, A. Yanovsky, J. Biol. Chem. 265 (1990) 20202–20209.
[19] S. Thennarasu, R. Nagaraj, Int. J. Pept. Protein Res. 46 (1995) 480–486.
[20] S. Thennarasu, R. Nagaraj, Protein Eng. 9 (1996) 1219–1224.
[21] Z. Oren, Y. Shai, Eur. J. Biochem. 237 (1996) 303–310.
[22] T.A. Holak, A. Engstrom, P.J. Kraulis, G. Lindeberg, H. Bennich, T.A. Jones, A.M. Gronenborn, G.M. Clore, Biochemistry 27 (1989) 7620–7629.
[23] D. Sipos, K. Chandrasekhar, K. Arvidsson, H. Engstrom, A. Ehrenberg, Eur. J. Biochem. 199 (1991) 285–291.
[24] J. Fink, A. Boman, H.G. Boman, R.B. Merrifield, Int. J. Pept. Protein Res. 33 (1989) 412–421.
[25] L.R. McLean, K.A. Hagaman, T.J. Owen, J.L. Krstenansky, Biochemistry 30 (1991) 31–37.
[26] S.E. Blondle, R.A. Houghten, Biochemistry 31 (1992) 12688–12694.
[27] R. Bessalle, A. Gorea, I. Shalit, J.W. Metzger, C. Dass, D.M. Desiderio, M. Fridkin, J. Med. Chem. 36 (1993) 1203–1209.
[28] G. Saberwal, R. Nagaraji, Biochim. Biophys. Acta 1197 (1994) 109–131.
[29] K. Matsuzaki, O. Murase, H. Tokuna, S. Funakoshi, N. Fujii, K. Miyajima, Biochemistry 33 (1994) 3342–3349.
[30] K. Matsuzaki, K. Sugishita, N. Fujii, K. Miyajima, Biochemistry 34 (1995) 3423–3429.
[31] M.M. Javadpour, M.M. Juban, W.-C. Lo, J.S.M. Bishop, J.B. Alberty, M. Cowell, C.L. Becker, M.L. McLaughlin, J. Med. Chem. 39 (1996) 3107–3113.
[32] R.E. Hancock, Lancet 349 (1997) 418–422.
[33] K. Matsuzaki, A. Nakamura, O. Murase, K. Sugishita, N. Fujii, K. Miyajima, Biochemistry 36 (1997) 2104–2111.
[34] K. Matsuzaki, K. Sugishita, N. Ishibe, M. Ueha, S. Nakata, K. Miyajima, R.M. Epand, Biochemistry 37 (1998) 11856–11863.
[35] R.B. Merrifield, Science 232 (1986) 341–347.
[36] S. Ohki, Biochim. Biophys. Acta 689 (1982) 1–11.
[37] N. Duzgunes, J. Wilschut, K. Hong, R. Fraley, C. Perry, D. Friend, T.L. James, P. Paphadjopoulos, Biochim. Biophys. Acta 732 (1983) 289–299.
[38] Y.-H. Chen, J.T. Yang, K.H. Chau, Biochemistry 13 (1974) 3350–3359.
[39] D. Oh, S.Y. Shin, J.H. Kang, K.-S. Hahm, Y. Kim, J. Pept. Res. 53 (1999) 578–589.
[40] T. Utsugi, A.J. Schroit, J. Connor, C.D. Bucana, I.J. Filder, Cancer Res. 51 (1991) 3062–3066.
[41] H.M. Chan, W. Wang, D. Smith, S.C. Chan, Biochim. Biophys. Acta 1336 (1997) 171–179.